

Activity model and chromatic effects on transit depths from ground-based multiband photometry

Manuel Perger

Institut d'Estudis Espacials de Catalunya (IEEC)
Institut de Ciències de l'Espai (ICE-CSIC)

Albert Rosich, Enrique Herrero

Matthias Mallonn

Ignasi Ribas, Juan Carlos Morales



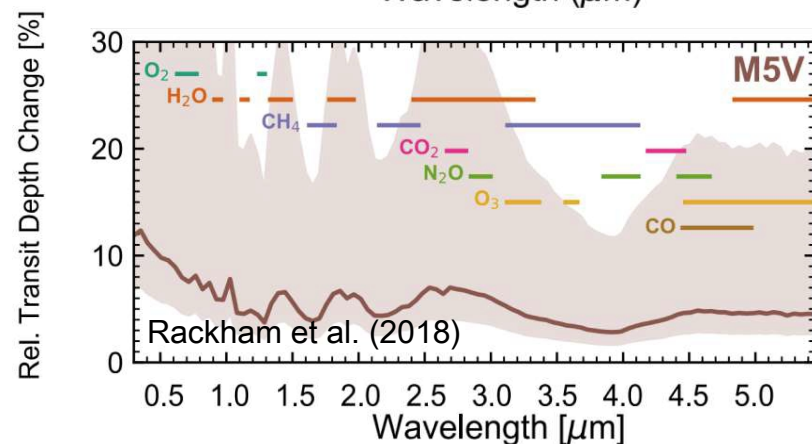
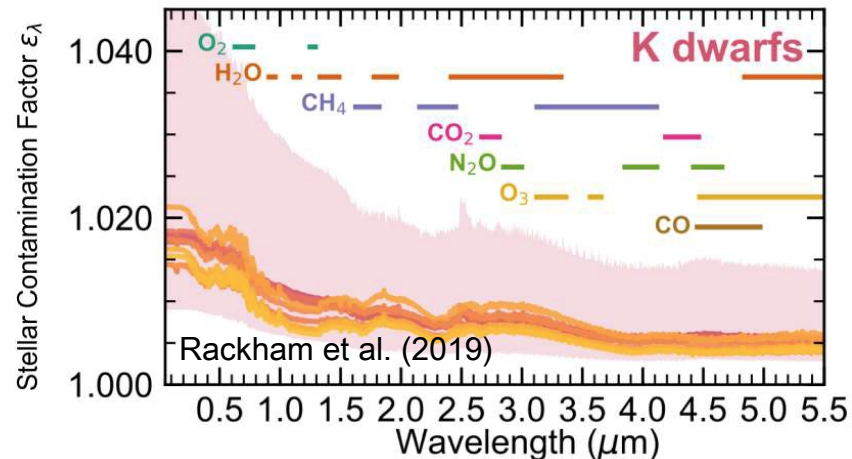
chromatic transit depth components

- limb darkening
- surface phenomena
- planet atmosphere

chromatic correction

photometric variation to estimate spot
filling factor and temperature contrast

$$\mathcal{D}'(\lambda) = \frac{\mathcal{D}_0}{1 - \delta_{\text{sp}} \left(1 - \frac{F_{\lambda, \text{sp}}}{F_{\lambda, \text{ph}}} \right)}$$



Activity model **F**

Set of stellar parameters θ

T_{eff} , P_{rot} , $\log(g)$, $[\text{Fe}/\text{H}]$, i

differential rotation

facula-to-spot Q

Grid of surface elements **S**

- immaculate photosphere, T_{ph}

- dark spots, T_{sp}

- bright faculae, T_{fac}

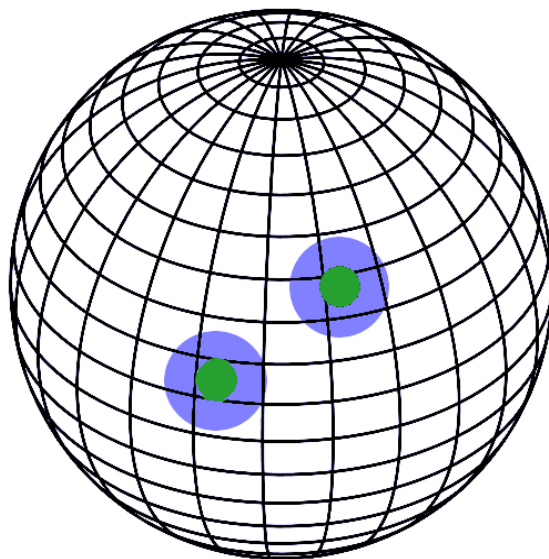
- t , dt , r , position

- Doppler shifts

- convective shifts

- limb darkening/brightening

- projection effects



Forward problem

$$\mathbf{X} = \mathbf{F}(\mathcal{S}, \theta) + \epsilon$$

Time-series data **X**

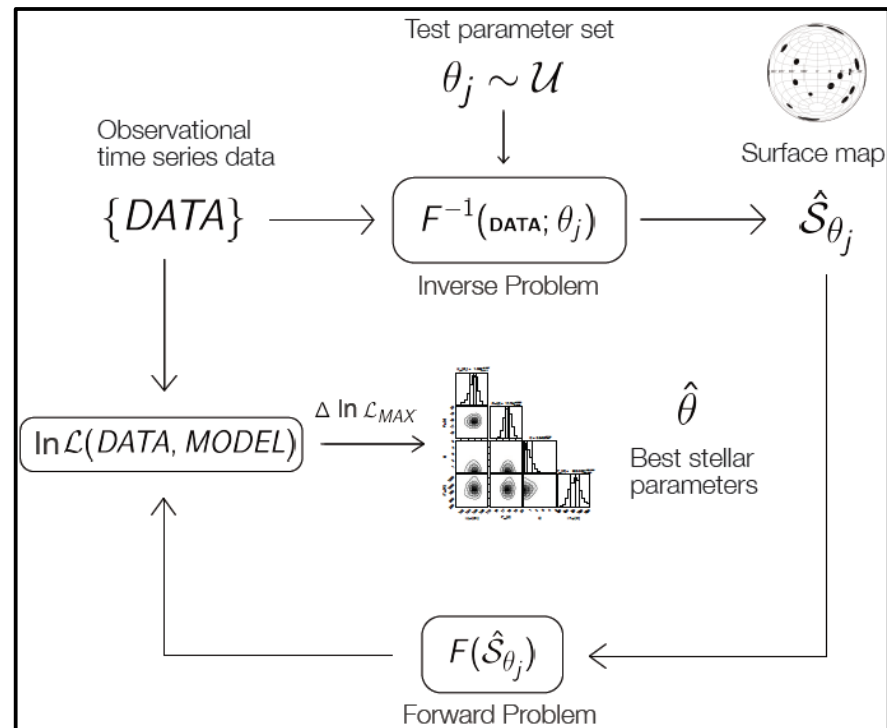
integrated over spectra or CCFs:
RV, photometry, activity indicators time series

$\hat{\mathcal{S}}_{\theta} = F^{-1}(\mathbf{X}, \theta)$
 \mathbf{S} surface map
 \mathbf{X} observables
 θ stellar parameters

$J(\mathcal{S}, \theta) = \sum_j^{\text{Obs.}} a_j \ln \mathcal{L}_j(\mathbf{X}_j | \mathcal{M}_j(\mathcal{S}, \theta))$
 J figure of merit
 \mathcal{M} STARSIM model

$$\mathcal{L}_j = \prod_i^N \frac{1}{\sqrt{2\pi}(\sigma_i^2 + s_j^2)} \exp\left[-\frac{(y_i - \mathcal{M}_{ij})^2}{2(\sigma_i^2 + s_j^2)}\right]$$

Monte Carlo simulated annealing optimization



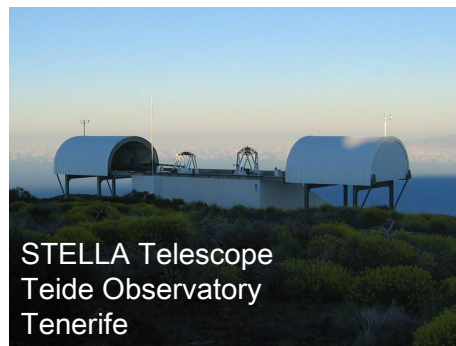
2 years of photometric observations

MEIA2 @ 0.8m Joan Oró; 536 *BR* obs.

WiFSIP @ 1.2m STELLA; 269 *BVI* obs.



Joan Oró Telescope (TJO)
Montsec Astronomical Observatory
Catalonia



STELLA Telescope
Teide Observatory
Tenerife

planet parameters

Hébrard+13; Louden+17; Mancini+17; May+18

Oshagh+18; Öztürk & Erdem+19

cloudy sodium-bearing atmosphere

Kirk+18; Louden+17; Chen+17; Alam+18

Table 1. Important parameters of WASP 52 (top) and WASP 52b (bottom).

parameter	unit	value	ref.
α	J2000	23:13:58.75	Ga18
δ	J2000	+08:45:39.9	Ga18
Sp.type	-	K2 V	He13
G	mag	$11.95^{0.13}_{0.36}$	Ga18
μ_α	mas a ⁻¹	-6.914±0.079	Ga18
μ_δ	mas a ⁻¹	-44.248±0.054	Ga18
Distance	pc	175.7±1.3	Ga18
M_*	M_\odot	0.81±0.05	Ma17
R_*	R_\odot	$0.860^{+0.021}_{-0.027}$	Ga18
L_*	L_\odot	0.4189±0.0046	Ga18
T_{eff}^a	K	5010^{+80}_{-60}	Ga18
$\log g^a$	cgs	4.582±0.014	He13
age	Ga	$0.4^{+0.3}_{-0.2}$	He13
$\log R'_{\text{HK}}$	cgs	-4.4±0.2	He13
λ	deg	$5.4^{4.6}_{-4.2}$	Öz18
M	M_J	0.46±0.02	He13
r	R_J	1.223±0.062	Öz19
P^b	days	1.7497828±0.0000006	Öz19
T_0^b	BJD	2405793.68128±0.00049	Öz19
r/R_*^b	-	0.159±0.0004	Öz19
b/R_*^b	-	0.60±0.02	He13
Orbit inc., i^b	deg	85.24±0.84	Öz19
a	au	0.0272±0.0003	He13

Notes. (a) fixed parameters in Section 3.3; (b) fixed parameters in Section 4;

References. He13: Hébrard et al. (2013); Ki16: Kirk et al. (2016); Ma17: Mancini et al. (2017); Os18: Oshagh et al. (2018); Ga18: Gaia Collaboration et al. (2018); Öz19 (Öztürk & Erdem 2019)

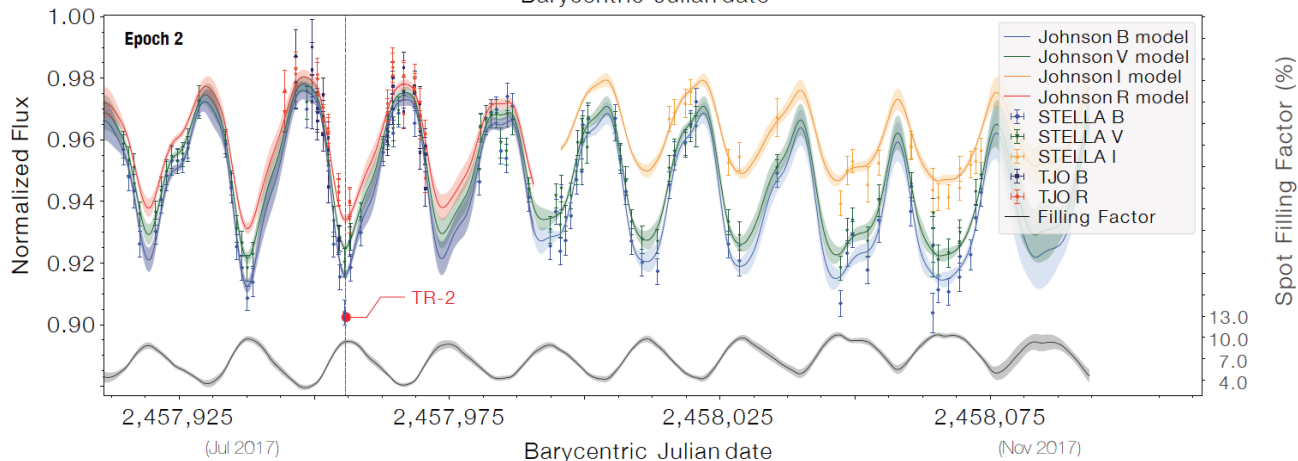
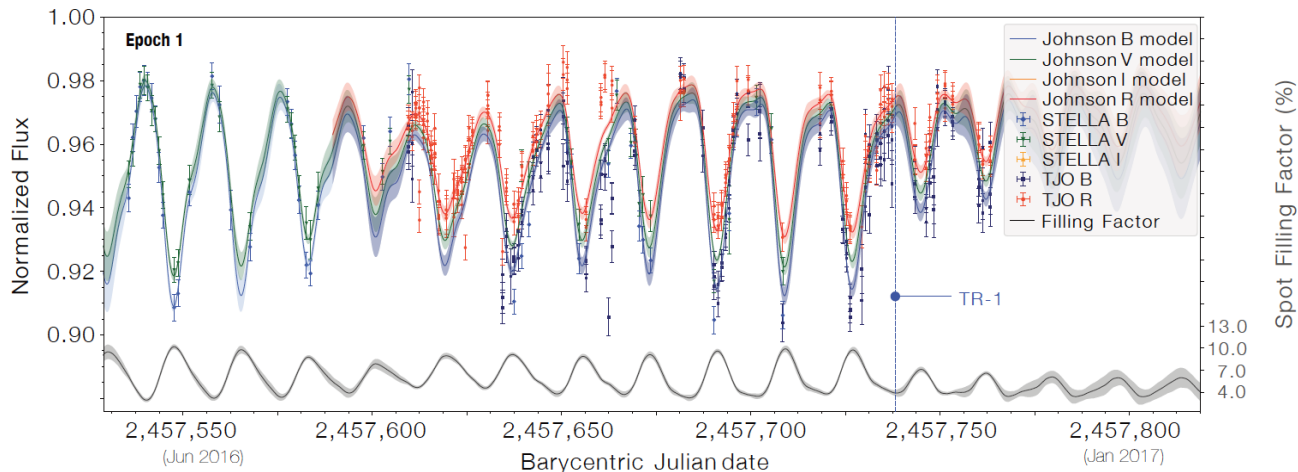
unocculted spots!

photometric variability 4-7%
filling factor 3-10%

example transits

TR-1: low-activity, ff=3%

TR-2: high-activity, ff=10%



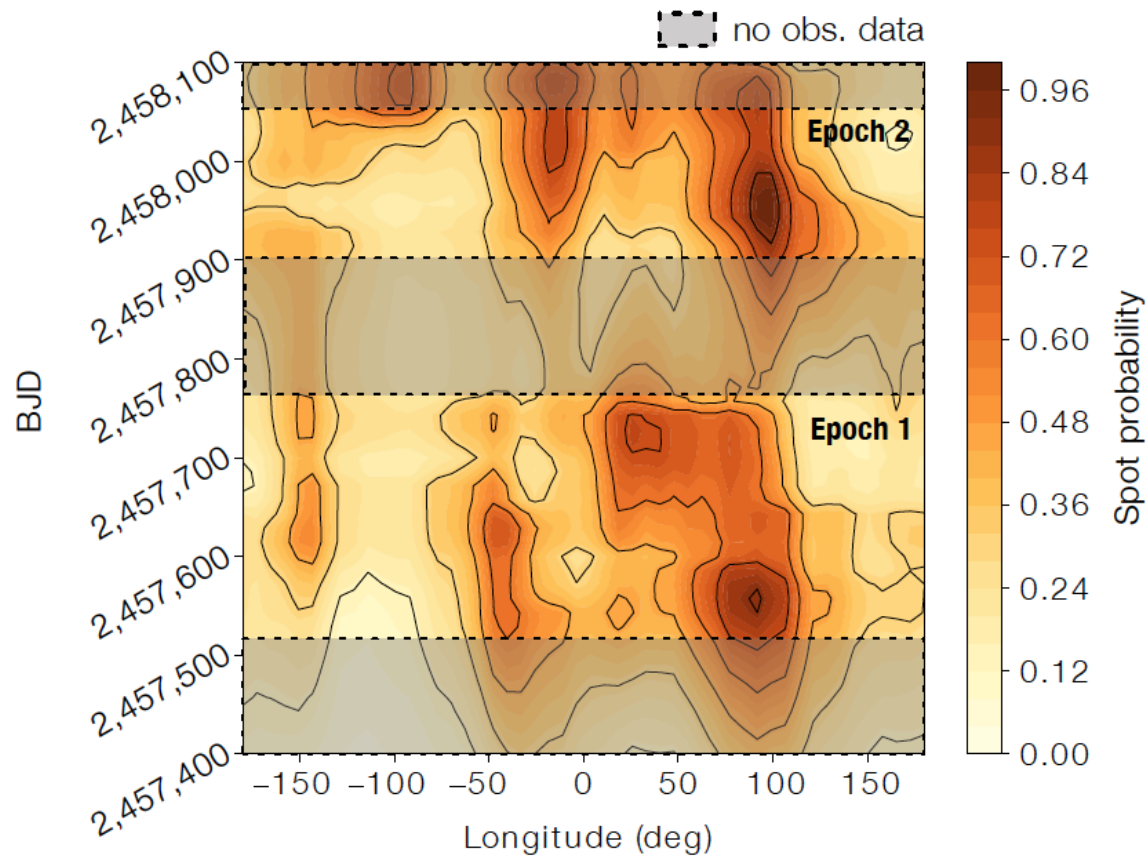
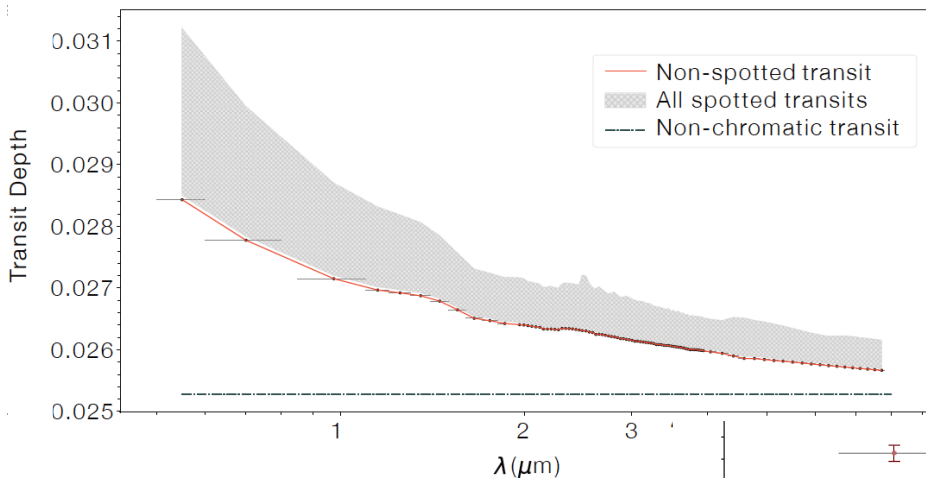


Table 2. Statistics of equivalently significant ~ 200 fitted StarSim parameters (top) and adjusted photometric offsets (bottom). As prior to the fitting process, the parameter values were uniformly distributed within their limits for all four parameters.

parameter	limits	value	ref.
P_{rot} (days)	[5, 50]	$17.75^{+0.33}_{-0.34}$	this work
		11.8 ± 3.3	He13
		15.53 ± 1.96	Ma17
		17.79 ± 0.05	Lo17
		18.06 ± 0.2	Br19
ΔT_{sp} (K)	[200, 2500]	825 ± 150	this work
		1250 - 1500	Ki16
		~ 270	Ma17
		~ 950	Br18
		250	Al18
		2230	Br19
Q^a	[0, 4]	$0.0^{+0.85}$	this work
$z_{\text{B,STELLA}}$	[0.98, 1.1]	$1.059^{+0.007}_{-0.011}$	this work
$z_{\text{V,STELLA}}$		$1.054^{+0.008}_{-0.012}$	this work ^b
$z_{\text{I,STELLA}}$		$1.047^{+0.005}_{-0.009}$	"
$z_{\text{B,TJO}}$		$1.051^{+0.007}_{-0.011}$	"
$z_{\text{R,TJO}}$		$1.041^{+0.007}_{-0.012}$	"

Notes. (a) Q is unilaterally distributed. (b) z_j calculated from the only fitted $z_{\text{B,STELLA}}$ proceeding as described in Sec. 3.3.2.

References. He13: Hébrard et al. (2013); Ki16: Kirk et al. (2016); Ma17: Mancini et al. (2017); Lo17: Louden et al. (2017); Al18: Alam et al. (2018); Br18: Bruno et al. (2018); Br19: Bruno et al. (2019)

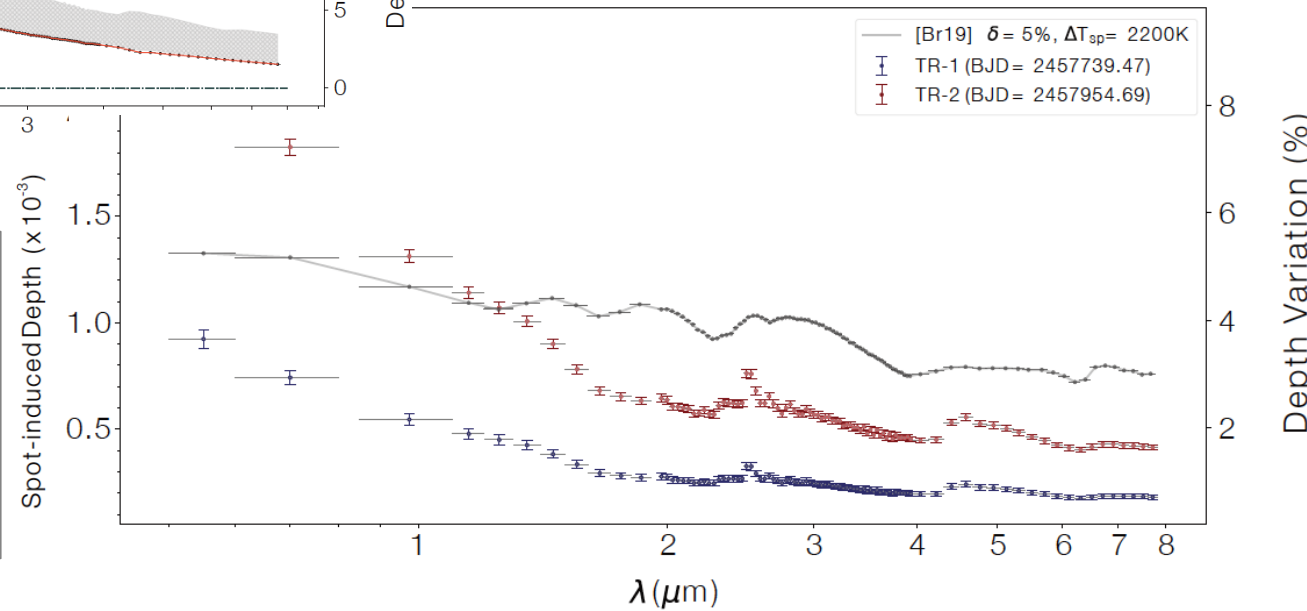


correction w/o STARSIM:
overestimation 3-11%

STARSIM correction:
overestimation < 0.5%

uncertainties

- photometric precision
- spot map variation



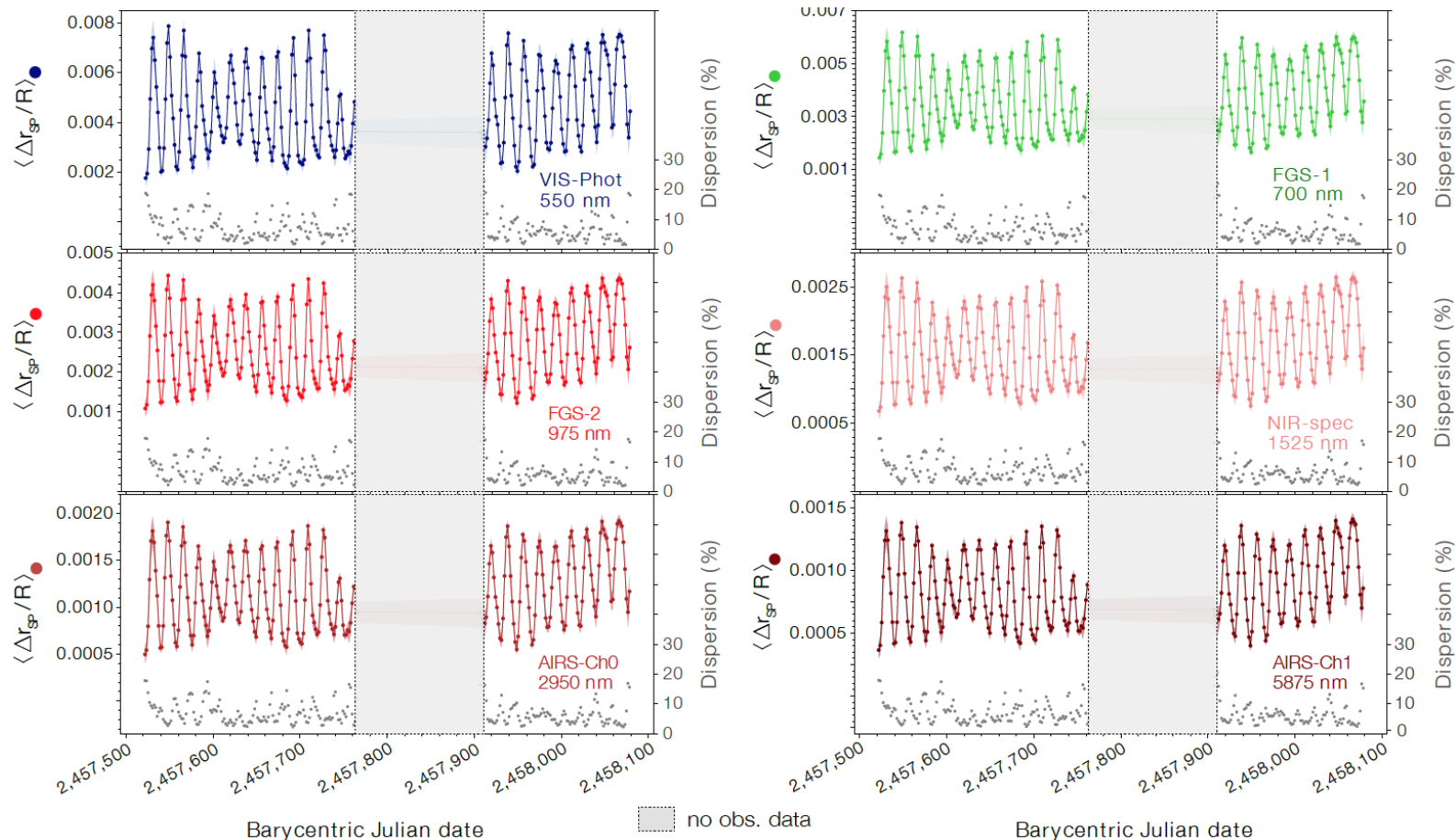
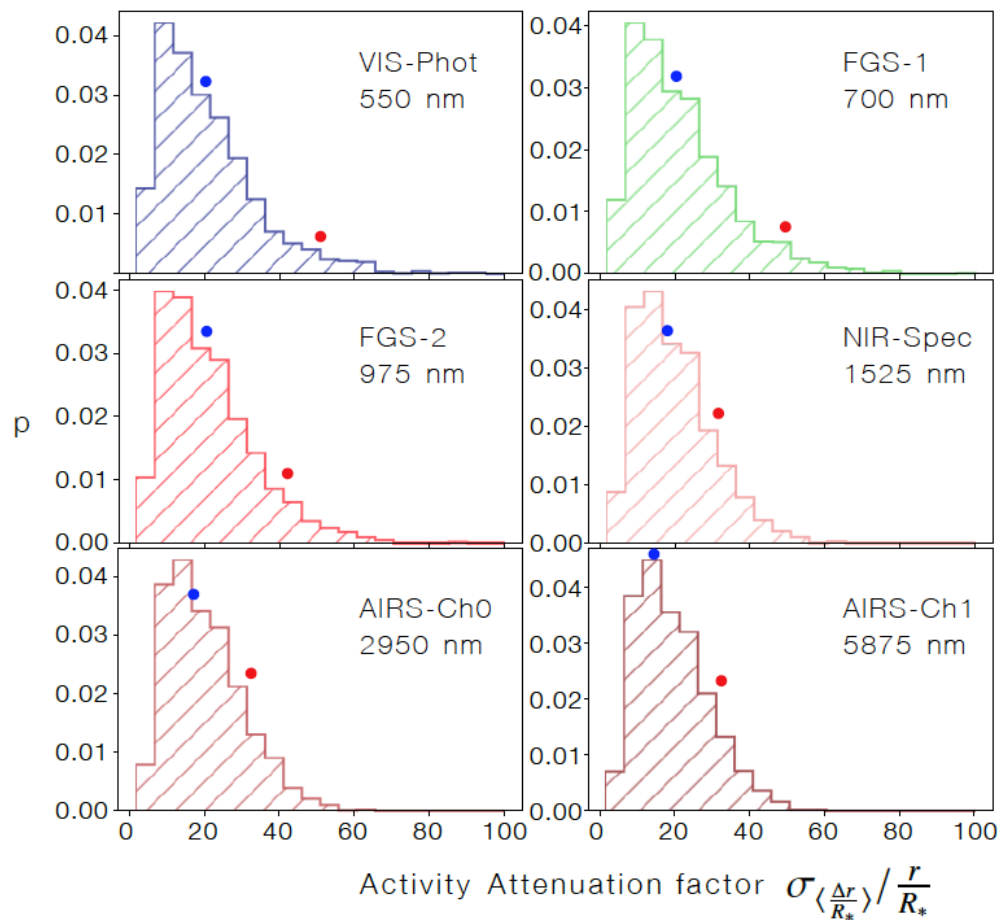


Table 3. Mean values of transit depth variations due to spots, $SP(\lambda)$, on WASP-52 simulated transits. The corresponding planet relative radius variations, $\frac{\Delta r_{SP}}{R_*}$, are also computed following Equation 12. Values for the low-activity transit TR-1 (top) and the high-activity transit TR-2 (bottom) cases are provided. λ_{eff} means the central wavelength of its corresponding channel.

Instrument	λ_{eff} (μm)	$\langle SP(\lambda) \rangle \pm \sigma$ ($\times 10^{-3}$)	$\langle \frac{\Delta r_{SP}}{R_*} \rangle \pm \sigma$ ($\times 10^{-3}$)
low-activity case TR-1			
VIS-Phot	0.55	0.92 ± 0.04	2.91 ± 0.13
FGS-1	0.7	0.74 ± 0.03	2.33 ± 0.10
FGS-2	0.975	0.54 ± 0.03	1.71 ± 0.08
NIR-Spec	1.525	0.33 ± 0.02	1.05 ± 0.06
AIRS-Ch0	2.95	0.25 ± 0.01	0.80 ± 0.04
AIRS-Ch1	5.875	0.18 ± 0.01	0.58 ± 0.04
high-activity case TR-2			
VIS-Phot	0.55	2.33 ± 0.04	7.32 ± 0.14
FGS-1	0.7	1.82 ± 0.04	5.72 ± 0.12
FGS-2	0.975	1.31 ± 0.03	4.12 ± 0.09
NIR-Spec	1.525	0.78 ± 0.02	2.45 ± 0.07
AIRS-Ch0	2.95	0.59 ± 0.02	1.86 ± 0.05
AIRS-Ch1	5.875	0.43 ± 0.01	1.35 ± 0.04



STARSIM and simultaneous multiband photometry

- independent filling factor and temperature contrast
- absolute filling factor
- precise stellar parameters and activity model
- activity correction factors of 5 to 30

Improvement with observational strategy and photometric precision

